Nonlinear frequency conversion in one dimensional lithium niobate photonic crystal nanocavities

Haowei Jiang, Hanxiao Liang, Rui Luo, Xianfeng Chen, Yuping Chen, and Qiang Lin

Citation: Appl. Phys. Lett. **113**, 021104 (2018); doi: 10.1063/1.5039948
View online: https://doi.org/10.1063/1.5039948
View Table of Contents: http://aip.scitation.org/toc/apl/113/2
Published by the American Institute of Physics

Nonlinear frequency conversion in one dimensional lithium niobate photonic crystal nanocavities

Haowei Jiang,[1,2,a)] Hanxiao Liang,[3,a)] Rui Luo,[2] Xianfeng Chen,[1] Yuping Chen,[1,b)] and Qiang Lin[2,3,b)]
[1]*State Key Laboratory of Advanced Optical Communication Systems and Networks, School of Physics and Astronomy, Shanghai Jiao Tong University, Shanghai 200240, China*
[2]*Institute of Optics, University of Rochester, Rochester, New York 14627, USA*
[3]*Department of Electrical and Computer Engineering, University of Rochester, Rochester, New York 14627, USA*

(Received 12 May 2018; accepted 27 June 2018; published online 12 July 2018)

We demonstrate flexible nonlinear frequency up-conversion in high-Q lithium niobate photonic crystal nanobeam resonators. The high optical Q together with strong optical mode confinement allows us to observe clear second harmonic generation and sum frequency generation with an optical power around only tens of microWatts. These demonstrations show that high-Q lithium niobate photonic crystal nanoresonators are of great promise for nonlinear photonic applications. *Published by AIP Publishing*. https://doi.org/10.1063/1.5039948

Lithium niobate (LN) exhibits a significant optical nonlinearity which has been applied for many important nonlinear and quantum photonic applications.[1–6] In general, nonlinear optical processes rely critically on the optical intensity, which can be dramatically increased by miniaturizing the device structure, leading to enhanced nonlinear conversion efficiency. This great potential has excited significant interest in recent years to explore nonlinear optics in on-chip LN photonic devices.[7–22] A photonic crystal nanocavity exhibits superior capability of confining light in subwavelength dimension; thus it is of great promise for nonlinear photonic application.[23–26] It, however, relies crucially on the optical quality of the device, which imposes a serious challenge for the LN platform.[27–37] Very recently, we have developed high-quality one-dimensional photonic crystal nanobeam resonators on the LN platform,[38] with optical Q up to $\sim 10^5$ while maintaining a small effective mode volume of $\sim (\frac{\lambda}{n})^3$. This development cleared up the technical obstacle for nonlinear photonic applications. In this paper, we utilize this type of device to demonstrate intriguing second harmonic generation (SHG) and sum frequency generation (SFG).

The device employed is a high Q one-dimensional photonic crystal nanocavity (Fig. 1), which is fabricated on an X-cut LN-on-insulator wafer, with a lattice constant of 545 nm. The suspended nanobeam has a thickness of 250 nm, with a 2-μm gap from the silicon substrate (Fig. 2, inset). The device structure was patterned using electron beam lithography and etched by an argon-ion milling process. The buried silica layer between the LN nanobeam and the silicon substrate was finally undercut by diluted hydrofluoric acid. More details about the device design and fabrication can be found in our previous paper.[38] The device was tested with the experimental setup shown in Fig. 2, where a tunable laser was launched into the photonic crystal nanocavity via a tapered optical fiber which also delivers the generated light output from the device. The up-converted light produced from the device is separated from the pump by a short pass filter before being recorded in a spectrometer. To prevent temperature-induced drift, the LN chip was placed on a thermoelectric cooler with a temperature stabilized at 27 °C.

The calibrated transmission is shown in Fig. 1. The device exhibits a single cavity mode over a broad telecom band, with an optical Q of 5.43×10^4 at the wavelength of 1504.7 nm. When we increased the input power to 310 μW and scanned the laser wavelength across the cavity resonance, the cavity transmission shows a clear therm-optic bistability [Fig. 3(a)], as expected.[39] Interestingly, when we scanned the laser wavelength into the cavity resonance, a bright spot appears in the center of the device where the nanocavity is located, as shown in Fig. 3(d). The spot becomes brighter when the laser wavelength falls deeper into the resonance, corresponding to increased optical power dropped into the

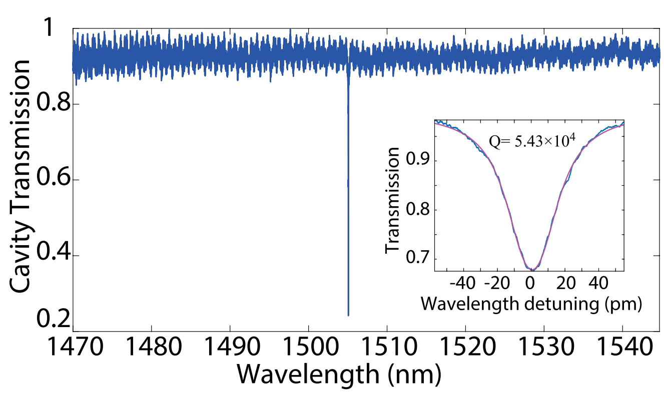

FIG. 1. Laser-scanned transmission spectrum of the LN photonic crystal nanobeam resonator used for second harmonic generation. The inset shows detailed transmission spectrum around the cavity resonance located at 1504.7 nm, with the experimental data shown in blue and the theoretical fitting shown in red. The cavity mode exhibits an intrinsic optical Q of 5.43×10^4.

[a)]H. Jiang and H. Liang contributed equally to this work.
[b)]Authors to whom correspondence should be addressed: ypchen@sjtu.edu.cn and qiang.lin@rochester.edu.

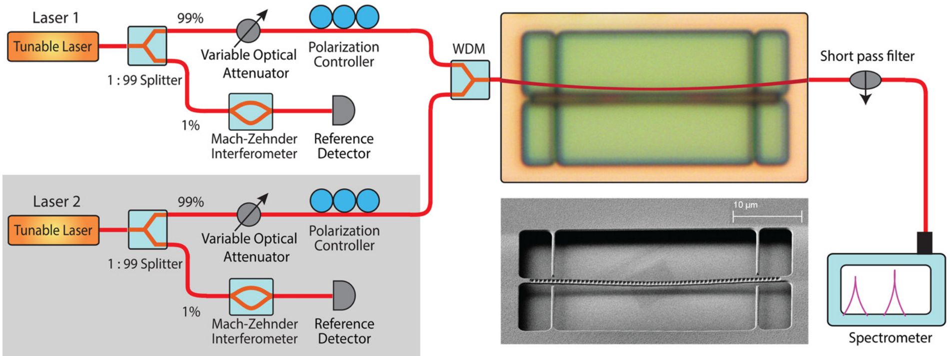

FIG. 2. Schematic of the experimental setup. The shaded area is applied only for the SFG process. The inset SEM image shows the real fabricated device. The pump lights are coupled into the nano-resonator via a tapered optical fiber which also delivers the produced SHG and SFG signal out of the device. The coupling efficiency is about 50% for the pump lights in the telecom band.

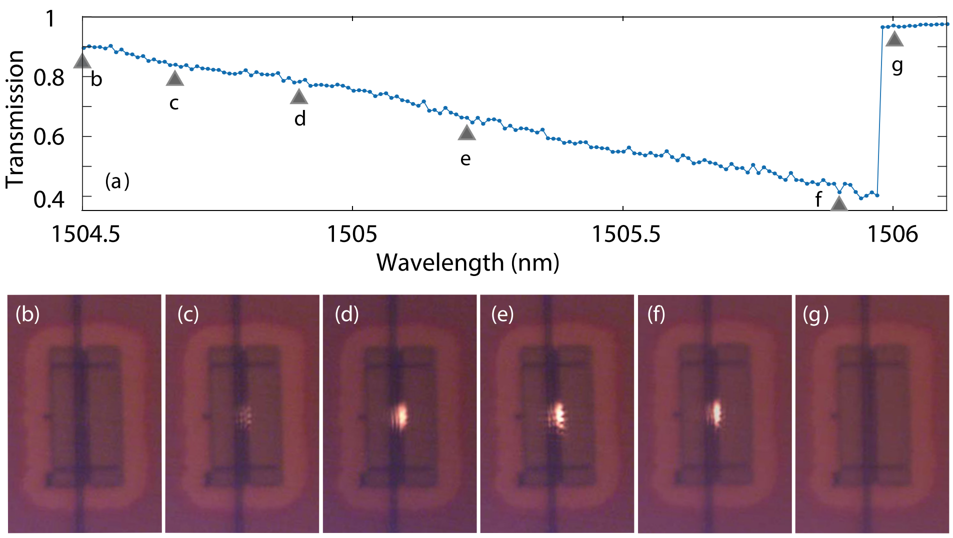

FIG. 3. (a) The transmission of the cavity with the input power of 310 μW (when the laser scans from blue to red across the cavity resonance). The dots show the experimentally recorded data, and the solid line is used for eye guidance only. (b)–(g) Optical microscopic images taken at different laser-cavity wavelength detunings as indicated in (a). The images were taken by a CMOS camera with a spectral range below 1100 nm.

cavity. Surprisingly, at a drop power of 80 μW, the spot is so bright [Fig. 3(d)] that it can be seen even by naked eyes.

As the imaging camera has a spectral response around visible and near infrared spectral range, the appearance of the bright spot implies the potential generation of second harmonic. To verify this, we recorded the spectrum of the emitted light. As shown in the inset of Fig. 4, a clear sharp spectral line appears at the wavelength of 752.8 nm, directly corresponding to the second harmonic of the pump wave at 1505.6 nm. To characterize the SHG process, we locked the laser wavelength half wave into the resonance and recorded the SHG power as a function of that of the fundamental wave, which is shown in Fig. 4. Figure 4 shows a clear quadratic power dependence, which further verify the second harmonic generation, since, as it is known, the SHG output intensity follows the equation $I_{2\omega} \propto d_{\rm eff}^2 I_\omega^2$, where $d_{\rm eff}$ is the effective nonlinear coefficient, and I_ω and $I_{2\omega}$ are the intensities of the fundamental wave and second harmonic, respectively. We recorded a nonlinear conversion efficiency of about 4×10^{-9}/mW for the second harmonic generation. The low efficiency is likely due to the low efficiency of coupling the second harmonic to the delivering tapered fiber which is not designed for use in this spectral range. The visibility of the bright spot shown in Fig. 3 to naked eyes indicates a potentially significant generation of the second harmonic. The reported high efficiencies in other lithium niobate wire beam structures also show great potential in improving the efficiency.[40,41] Future optimization of the external coupling of the second harmonic wave would help improve the collection efficiency.

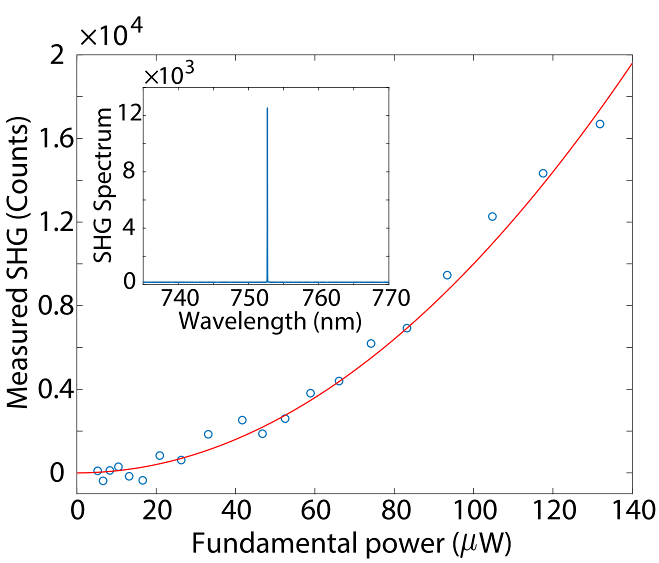

FIG. 4. Recorded power dependence of the second harmonic signal as a function of the power dropped into the fundamental cavity mode. The inset shows the emission spectrum of the second harmonic.

To demonstrate a SFG process, we select another device with a lattice constant of 520 nm. The change of lattice constant shifts the photonic band gap of the device. As a result, two optical modes appears in the telecom spectral range 1470–1540 nm, as shown clearly in the cavity transmission spectrum in Fig. 5(a). The two cavity modes exhibit similar

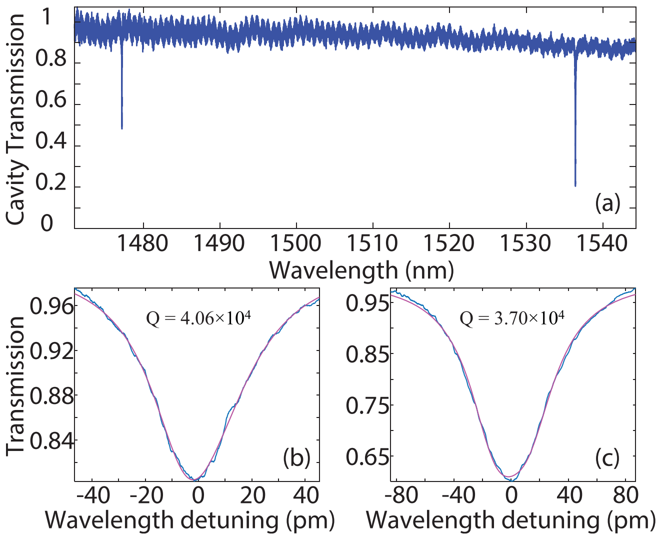

FIG. 5. (a) Laser-scanned transmission spectrum of the device used for sum-frequency generation. (b) and (c) Detailed transmission spectra of the two cavity modes located at 1477.1 nm (Mode 1) and 1536.6 nm (Mode 2), respectively, with experimental data shown in blue and theoretical fitting shown in red. The Mode 1 and Mode 2 exhibit intrinsic optical Qs of 4.06×10^4 and 3.70×10^4, respectively.

high optical Q and have a spatial overlap of about 40%. As shown in the detailed transmission spectra in Figs. 5(b) and 5(c), the cavity mode 1 at 1477.1 nm exhibits an optical Q of 4.06×10^4, while the mode 2 at 1536.6 nm exhibits an optical Q of 3.70×10^4. To show the SFG phenomena, we launched one laser (Laser 1) at 1477.1 nm into the cavity mode 1 and added a second laser (Laser 2) at 1536.6 nm to the testing setup (Fig. 2) which was launched into the cavity mode 2. The two lasers were combined together with a wavelength-division multiplexing filter and then launched into the device.

We increased the powers of the lasers and monitored the emission spectrum around the second harmonic wavelengths. As shown in Fig. 6(a), three sharp spectral lines appear clearly. The left line locates at the wavelength of 738.6 nm, directly corresponding to the second harmonic of the pump mode 1, while the right line at 768.3 nm corresponding to the second harmonic of the pump mode 2. The central line at the wavelength of 753.2 nm exactly meets the energy conservation of the SFG process. The amplitude of the SFG spectral line grows with the power increasing of either one or both of the two pump modes. By mapping out the power of the sum frequency spectral components as a function of the optical powers of the two lasers, we obtain Fig. 6(b) which plots the power of sum frequency component as a function of the product of the two laser powers. It clearly shows a linear dependence, which agrees well with the theoretical expectation of $I_{SFG} \propto d_{eff}^2 I_1 \cdot I_2$.

In conclusion, we have demonstrated second harmonic generation and sum frequency generation in high-Q lithium niobate photonic crystal nanobeam resonators. We performed detailed characterizations of the spectral characteristics and the associated power dependence, which agree well with the theoretical expectation. The demonstration of flexible nonlinear frequency conversion in these devices shows great promise of nonlinear photonic applications using high-Q LN photonic crystal nanoresonators.

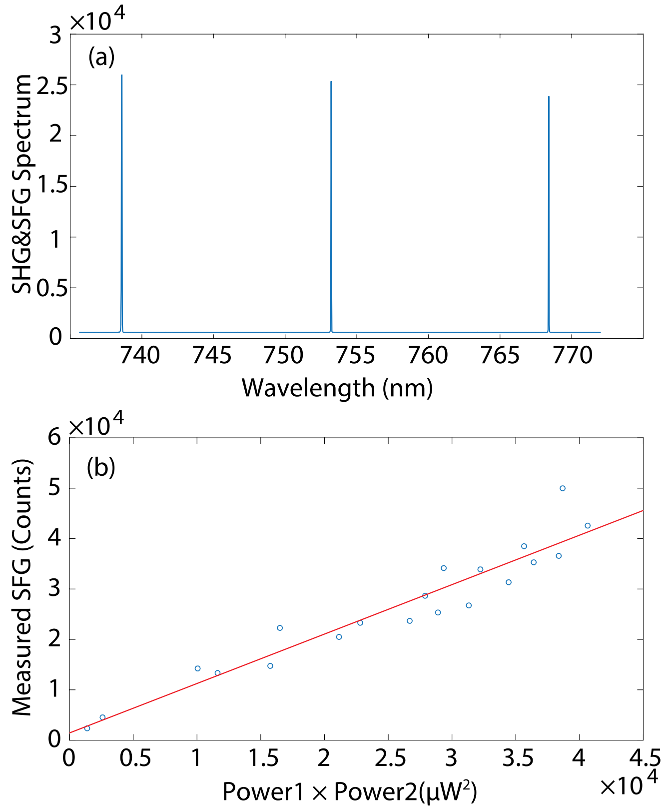

FIG. 6. (a) Emission spectrum when we launched simultaneously the two lasers into the two cavity modes. (b) Recorded power dependence of the spectral component at the sum frequency, as a function of the product of the laser powers dropped into the two cavity modes shown in Fig. 5(a). The blue circles show the experimental data, and the red line shows a linear fitting to the data.

This work was supported by the National Natural Science Foundation of China (NSFC) (11574208 and 61235009), the National Key R&D Program of China (2017YFA0303700), and the National Science Foundation (NSF) (ECCS-1509749 and EFRI-1641099). It was performed in part at the Cornell NanoScale Facility, a member of the National Nanotechnology Coordinated Infrastructure (NNCI).

[1]R. S. Weis and T. K. Gaylord, “Lithium niobate: Summary of physical properties and crystal structure,” Appl. Phys. A **37**, 191–203 (1985).
[2]L. E. Myers, R. C. Eckardt, M. M. Fejer, R. L. Byer, W. R. Bosenberg, and J. W. Pierce, “Quasi-phase-matched optical parametric oscillators in bulk periodically poled linbo3,” J. Opt. Soc. Am. B **12**, 2102–2116 (1995).
[3]S. Tanzilli, H. De Riedmatten, W. Tittel, H. Zbinden, P. Baldi, M. De Micheli, D. B. Ostrowsky, and N. Gisin, “Highly efficient photon-pair source using periodically poled lithium niobate waveguide,” Electron. Lett. **37**, 26–28 (2001).
[4]Y. Lee, F. Fan, Y. C. Huang, B. Gu, B. Dong, and M. Chou, “Nonlinear multiwavelength conversion based on an aperiodic optical superlattice in lithium niobate,” Opt. Lett. **27**, 2191–2193 (2002).
[5]M. Halder, A. Beveratos, N. Gisin, V. Scarani, C. Simon, and H. Zbinden, “Entangling independent photons by time measurement,” Nat. Phys. **3**, 692–695 (2007).
[6]J. Zhang, Y. Chen, F. Lu, and X. Chen, “Flexible wavelength conversion via cascaded second order nonlinearity using broadband shg in mgo-doped ppln,” Opt. Express **16**, 6957 (2008).
[7]G. Poberaj, H. Hu, W. Sohler, and P. Günter, “Lithium niobate on insulator (lnoi) for micro-photonic devices,” Laser Photonics Rev. **6**, 488–503 (2012).

[8]T.-J. Wang, J.-Y. He, C.-A. Lee, and H. Niu, "High-quality linbo3 microdisk resonators by undercut etching and surface tension reshaping," Opt. Express **20**, 28119–28124 (2012).
[9]P. Rabiei, J. Ma, S. Khan, J. Chiles, and S. Fathpour, "Heterogeneous lithium niobate photonics on silicon substrates," Opt. Express **21**, 25573–25581 (2013).
[10]C. Wang, M. J. Burek, Z. Lin, H. A. Atikian, V. Venkataraman, I. C. Huang, P. Stark, and M. Loncar, "Integrated high quality factor lithium niobate microdisk resonators," Opt. Express **22**, 30924–30933 (2014).
[11]J. Lin, Y. Xu, Z. Fang, M. Wang, J. Song, N. Wang, L. Qiao, W. Fang, and Y. Cheng, "Fabrication of high-q lithium niobate microresonators using femtosecond laser micromachining," Sci. Rep. **5**, 8072 (2015).
[12]R. Geiss, S. Saravi, A. Sergeyev, S. Diziain, F. Setzpfandt, F. Schrempel, R. Grange, E. B. Kley, A. Tünnermann, and T. Pertsch, "Fabrication of nanoscale lithium niobate waveguides for second-harmonic generation," Opt. Lett. **40**, 2715–2718 (2015).
[13]F. Bo, J. Wang, J. Cui, S. K. Ozdemir, Y. Kong, G. Zhang, J. Xu, and L. Yang, "Lithium-niobate–silica hybrid whispering-gallery-mode resonators," Adv. Mater. **27**, 8075–8081 (2015).
[14]P. O. Weigel, M. Savanier, C. T. DeRose, A. T. Pomerene, A. L. Starbuck, A. L. Lentine, V. Stenger, and S. Mookherjea, "Lightwave circuits in lithium niobate through hybrid waveguides with silicon photonics," Sci. Rep. **6**, 22301 (2016).
[15]W. C. Jiang and Q. Lin, "Chip-scale cavity optomechanics in lithium niobate," Sci. Rep. **6**, 36920 (2016).
[16]L. Chang, Y. Li, N. Volet, L. Wang, J. Peters, and J. E. Bowers, "Thin film wavelength converters for photonic integrated circuits," Optica **3**, 531–535 (2016).
[17]L. Chang, M. H. Pfeiffer, N. Volet, M. Zervas, J. D. Peters, C. L. Manganelli, E. J. Stanton, Y. Li, T. J. Kippenberg, and J. E. Bowers, "Heterogeneous integration of lithium niobate and silicon nitride waveguides for wafer-scale photonic integrated circuits on silicon," Opt. Lett. **42**, 803–806 (2017).
[18]A. Rao, J. Chiles, S. Khan, S. Toroghi, M. Malinowski, G. F. Camacho-González, and S. Fathpour, "Second-harmonic generation in single-mode integrated waveguides based on mode-shape modulation," Appl. Phys. Lett. **110**, 111109 (2017).
[19]C. Wang, X. Xiong, N. Andrade, V. Venkataraman, X.-F. Ren, G.-C. Guo, and M. Lončar, "Second harmonic generation in nano-structured thin-film lithium niobate waveguides," Opt. Express **25**, 6963–6973 (2017).
[20]R. Wolf, I. Breunig, H. Zappe, and K. Buse, "Cascaded second-order optical nonlinearities in on-chip micro rings," Opt. Express **25**, 29927–29933 (2017).
[21]C. Wang, Z. Li, M.-H. Kim, X. Xiong, X.-F. Ren, G.-C. Guo, N. Yu, and M. Lončar, "Metasurface-assisted phase-matching-free second harmonic generation in lithium niobate waveguides," Nat. Commun. **8**, 2098 (2017).
[22]A. Boes, B. Corcoran, C. Lin, J. Bowers, and A. Mitchell, "Status and potential of lithium niobate on insulator (lnoi) for photonic integrated circuits," Laser Photonics Rev. **12**, 1700256 (2018).
[23]S. Noda, M. Fujita, and T. Asano, "Spontaneous-emission control by photonic crystals and nanocavities," Nat. Photonics **1**, 449 (2007).
[24]P. Lalanne, C. Sauvan, and J. P. Hugonin, "Photon confinement in photonic crystal nanocavities," Laser Photonics Rev. **2**, 514–526 (2008).
[25]M. Notomi, "Manipulating light with strongly modulated photonic crystals," Rep. Prog. Phys. **73**, 096501 (2010).
[26]J. D. Joannopoulos, S. G. Johnson, J. N. Winn, and R. D. Meade, *Photonic Crystals: Molding the Flow of Light* (Princeton University Press, 2011).
[27]M. Roussey, M.-P. Bernal, N. Courjal, and F. I. Baida, "Experimental and theoretical characterization of a lithium niobate photonic crystal," Appl. Phys. Lett. **87**, 241101 (2005).
[28]G. Zhou and M. Gu, "Direct optical fabrication of three-dimensional photonic crystals in a high refractive index linbo3 crystal," Opt. Lett. **31**, 2783–2785 (2006).
[29]M. Roussey, M.-P. Bernal, N. Courjal, D. Van Labeke, F. Baida, and R. Salut, "Electro-optic effect exaltation on lithium niobate photonic crystals due to slow photons," Appl. Phys. Lett. **89**, 241110 (2006).
[30]F. Sulser, G. Poberaj, M. Koechlin, and P. Günter, "Photonic crystal structures in ion-sliced lithium niobate thin films," Opt. Express **17**, 20291–20300 (2009).
[31]R. Geiss, S. Diziain, R. Iliew, C. Etrich, H. Hartung, N. Janunts, F. Schrempel, F. Lederer, T. Pertsch, and E.-B. Kley, "Light propagation in a free-standing lithium niobate photonic crystal waveguide," Appl. Phys. Lett. **97**, 131109 (2010).
[32]N. Courjal, S. Benchabane, J. Dahdah, G. Ulliac, Y. Gruson, and V. Laude, "Acousto-optically tunable lithium niobate photonic crystal," Appl. Phys. Lett. **96**, 131103 (2010).
[33]N. Courjal, J. Dahdah, G. Ulliac, P. Sevillano, B. Guichardaz, and F. Baida, "Optimization of linbo 3 photonic crystals: Toward 3d linbo 3 micro-components," Opt. Express **19**, 23008–23016 (2011).
[34]H. Lu, F. Issam Baida, G. Ulliac, N. Courjal, M. Collet, and M.-P. Bernal, "Lithium niobate photonic crystal wire cavity: Realization of a compact electro-optically tunable filter," Appl. Phys. Lett. **101**, 151117 (2012).
[35]S. Diziain, R. Geiss, M. Zilk, F. Schrempel, E.-B. Kley, A. Tünnermann, and T. Pertsch, "Second harmonic generation in free-standing lithium niobate photonic crystal l3 cavity," Appl. Phys. Lett. **103**, 051117 (2013).
[36]R. Geiss, S. Diziain, M. Steinert, F. Schrempel, E.-B. Kley, A. Tünnermann, and T. Pertsch, "Photonic crystals in lithium niobate by combining focussed ion beam writing and ion-beam enhanced etching," Phys. Status Solidi A **211**, 2421–2425 (2014).
[37]L. Cai, H. Han, S. Zhang, H. Hu, and K. Wang, "Photonic crystal slab fabricated on the platform of lithium niobate-on-insulator," Opt. Lett. **39**, 2094–2096 (2014).
[38]H. Liang, R. Luo, Y. He, H. Jiang, and Q. Lin, "High-quality lithium niobate photonic crystal nanocavities," Optica **4**, 1251–1258 (2017).
[39]T. Carmon, L. Yang, and K. J. Vahala, "Dynamical thermal behavior and thermal self-stability of microcavities," Opt. Express **12**, 4742–4750 (2004).
[40]S. Kurimura, Y. Kato, M. Maruyama, Y. Usui, and H. Nakajima, "Quasi-phase-matched adhered ridge waveguide in linbo3," Appl. Phys. Lett. **89**, 191123 (2006).
[41]R. Kou, S. Kurimura, K. Kikuchi, A. Terasaki, H. Nakajima, K. Kondou, and J. Ichikawa, "High-gain, wide-dynamic-range parametric interaction in mg-doped linbo3 quasi-phase-matched adhered ridge waveguide," Opt. Express **19**, 11867–11872 (2011).